Journal of Organometallic Chemistry 693 (2008) 3851–3857

Contents lists available at ScienceDirect

Journal of Organometallic Chemistry

journal homepage: www.elsevier.com/locate/jorganchem

Preparation, characterization, and catalytic properties of ruthenium nitrosyl complexes with polypyrazolylmethane ligands

Hui-Jun Xu [a], Yong Cheng [a], Jia-Feng Sun [a], Brenda A. Dougan [b], Yi-Zhi Li [a], Xue-Tai Chen [a,*], Zi-Ling Xue [b]

[a] Coordination Chemistry Institute, State Key Laboratory of Coordination Chemistry, Nanjing National Laboratory of Microstructures, School of Chemistry and Chemical Engineering, Nanjing University, Nanjing 210093, PR China
[b] Department of Chemistry, University of Tennessee, Knoxville, TN 37996-1600, USA

ARTICLE INFO

Article history:
Received 27 August 2008
Received in revised form 24 September 2008
Accepted 25 September 2008
Available online 2 October 2008

Keywords:
Ruthenium(II)
Nitrosyl
Polypyrazolylmethane
Catalyst
Transfer
Hydrogenation

ABSTRACT

Ruthenium(II) nitrosyl complexes with polypyrazolylmethanes, [(Bpm)Ru(NO)Cl_3] [Bpm = bis(1-pyrazolyl)methane, **1**], [(Bpm*)Ru(NO)Cl_3] [Bpm* = bis(3,5-dimethyl-1-pyrazolyl)methane, **2**], [(Tpm)Ru(NO)Cl_2][PF_6] [Tpm = tris(1-pyrazolyl)methane, **3**], and [(Tpm*)Ru(NO)Cl_2][PF_6] [Tpm* = tris(3,5-dimethyl-1-pyrazolyl)methane, **4**], have been synthesized and characterized. The solid-state structures of [(Bpm*)Ru(NO)Cl_3] (**2**) and [(Tpm*)Ru(NO)Cl_2][PF_6] (**4**) were determined by single-crystal X-ray crystallographic analyses. These complexes have been tested as catalysts in the transfer hydrogenation of several ketones under mild conditions.

© 2008 Elsevier B.V. All rights reserved.

1. Introduction

Metal nitrosyl complexes have attracted much research interest due to the specific interactions between metal ions and the nitrosyl ligand [1–6]. As a family of important metal nitrosyls, ruthenium nitrosyl complexes have been extensively studied over the years for their novel reactivities and biological and environmental significance [7]. Recently some ruthenium nitrosyl complexes have been found to be catalyst precursors in hydrogenation of cyclohexene [8], hydrogenation of carbon dioxide and dicarbonate [9], isomerization of olefin [10], and methylenation of aldehydes [11].

Catalytic transfer hydrogenation employing hydrogen donors, e.g. 2-propanol is safer, highly selective, economic, and eco-friendly. A broad range of alcohols are accessible by transfer hydrogenation under mild reactions in the presence of various metal catalysts [12,13]. A large number of ruthenium complexes have been reported as catalyst precursors for transfer hydrogenation of ketones and shown high activity [12–16]. Most of the reported ruthenium catalysts are based on phosphine-containing ligands. Recently ruthenium complexes supported by polydentate nitrogen ligands have been found to be very effective transfer hydrogenation catalyst to reduction of ketone [17–21]. To the best of our knowledge, there has been no report of ruthenium nitrosyl complexes used in this particular transformation to date.

Polypyrazolyborate ligands have proved to be versatile ligands used in coordination and organometallic chemistry [22,23]. Ruthenium complexes bearing bis(pyrazolyl)borate (Bp) and tris(pyrazolyl)borate (Tp) ligands have attracted considerable research attentions [24–27]. However, only a limited number of ruthenium nitrosyl complexes with polypyrazolyborate ligands have been reported [28–35]. Onishi et al. have reported the preparation and novel reactivities of the ruthenium nitrosyls bearing Tp ligand and their alkynyl derivatives [28–35]. Polypyrazolylmethanes, such as bis(3,5-dimethyl-1-pyrazolylmethane) (Bpm*) and tris(1-pyrazolyl)methane (Tpm), are the neutral analogues of the Bp and Tp ligands [36,37], which are isosteric and isoelectronic with the anionic polypyrazolyborates. Ruthenium complexes with Bpm and Tpm and their derivatives have also been prepared [38–43]. However ruthenium nitrosyl complexes of polypyrazolylmethanes are scarcely studied. To the best of our knowledge, only two such complexes have been reported [28,44]. Onishi has reported the synthesis of {(Pz_2CMe_2)$RuCl_3$(NO)} {Pz_2CMe_2 = 2,2-bis(1-pyrazolyl)propane} [28]. Olabe et al. [44] have prepared a novel ruthenium nitrosyl complex with Tpm and bippyridine and studied the reactivities of the bound NO ligand. In this paper, we report the synthesis and characterization of ruthenium(II) nitrosyl complexes with

* Corresponding author. Tel./fax: +86 25 83314502.
E-mail address: xtchen@netra.nju.edu.cn (X.-T. Chen).

0022-328X/$ - see front matter © 2008 Elsevier B.V. All rights reserved.
doi:10.1016/j.jorganchem.2008.09.045

polypyrazolylmethanes, [(Bpm)Ru(NO)Cl_3] (**1**), [(Bpm*)Ru(NO)Cl_3] (**2**), [(Tpm)Ru(NO)Cl_2][PF_6] (**3**) and [(Tpm*)Ru(NO)Cl_2][PF_6] (**4**). These complexes have been found to be catalysts for hydrogenation transfer of ketones in a basic 2-propanol solution

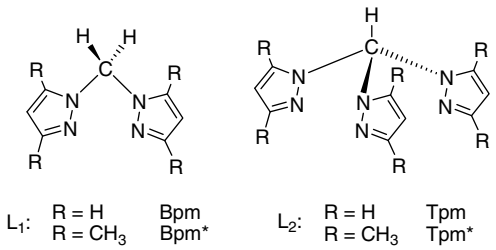

.

2. Experimental

2.1. Reagents and general techniques

All manipulations were performed under an inert atmosphere of dry nitrogen using standard Schlenk techniques. Solvents were purified by standard methods and stored under nitrogen. Bpm [45], Bpm* [45], Tpm [46], Tpm* [46], and Ru(NO)$Cl_3 \cdot 5H_2O$ [47] were prepared as described in the literature. All other reagents were obtained commercially and used without further purification.

2.2. Physical measurements

The analysis of carbon, hydrogen and nitrogen were made on a Perkin–Elmer 240C element analyzer. Infrared (IR) spectra were recorded on a Bruker Vetor 22 Fourier Transform (FT)-IR spectrophotometer by using KBr disks in the range 4000–400 cm^{-1}. NMR spectra at room temperature were recorded either on a Bruker DRX500 at 500 MHz (^{1}H) and 125 MHz (^{13}C) or on a Bruker AMX-400 spectrometer at 400 MHz (^{1}H) and 100 MHz (^{13}C). Variable-temperature ^{1}H NMR spectra were recorded on the Bruker AMX-400 spectrometer. The NMR spectra were referenced to $SiMe_4$ or solvent (residual protons in the ^{1}H spectra). Electrochemical measurements were made on a 273A Potentiostat/Gawanostat (EG&G) using a glassy carbon working electrode, a platinum wire counter electrode, and Bu_4NClO_4 (TBAP) as Supporting electrolyte. All the potentials were referenced to SSCE electrode and the solutions were purged with N_2 before each set of experiments.

2.3. Synthesis of [(L_1)Ru(NO)Cl_3] [L_1 = Bpm (**1**), Bpm* = (**2**)]

A solution of Bpm or Bpm* (0.55 mmol) and Ru(NO)$Cl_3 \cdot 5H_2O$ (0.164 g, 0.5 mmol) in methanol (15 ml) was heated under reflux for 1 h. The resultant pale pink solids were filtered from the cooled solution and washed with hot methanol and then diethyl ether, and dried under reduced pressure. A reaction between Bpm* and Ru(NO)$Cl_3 \cdot 5H_2O$ at 80 °C gave the suitable crystals of **2**.

1: Yield: 0.170 g, 88% based on Ru(NO)$Cl_3 \cdot 5H_2O$. Anal. Calc. for $RuC_7H_8Cl_3N_5O$: C, 21.80; H, 2.09; N, 18.16. Found: C, 21.88; H, 2.03; N, 18.23%. IR (KBr, cm^{-1}): ν(NO) = 1870. ^{1}H NMR (DMSO-d_6, 298 K): δ 6.63 (d, 1H, $^2J_{H-H}$ = 14.75 Hz, CH_2), 6.73 (pseudo-t, 2H, 4-*H*), 7.14 (d, 1H, $^2J_{H-H}$ = 14.8 Hz, CH_2), 8.24 (d, 2H, 3 or 5-*H*), 8.36 (d, 2H, 3 or 5-*H*).

2: Yield: 0.154 g, 70% based on Ru(NO)$Cl_3 \cdot 5H_2O$. Anal. Calc. for $RuC_{11}H_{16}Cl_3N_5O$: C, 29.91; H, 3.65; N, 15.86. Found: C, 30.01; H, 3.69; N, 15.69%. IR (KBr, cm^{-1}): ν(NO) = 1875. ^{1}H NMR (DMF-d_7, 298 K): δ 2.64 (s, 3H, 3 or 5-CH_3), 2.76 (s, 3H, 3 or 5-CH_3), 6.32 (s, 2H, 4-*H*), 6.57 (d, 1H, $^2J_{H-H}$ = 16.55 Hz, CH_2), 6.85 (br, 1H, CH_2). ^{13}C{H} NMR (DMF-d_7, 298 K): δ 157.35 (*C*3), 144.80 (*C*5), 110.22 (*C*4), 58.37 (CH_2), 15.08 (3-CH_3), 11.40 (5-CH_3).

2.4. Synthesis of [(Tpm)Ru(NO)Cl_2][PF_6] (**3**)

Tpm (0.235 g, 1.1 mmol) was added to a solution of Ru(NO)$Cl_3 \cdot 5H_2O$ (0.328 g, 1.0 mmol) in C_2H_5OH–H_2O (3:1 v/v; 30 ml). This mixture was refluxed for 2 h to give a reddish-brown solution, which was then cooled to room temperature. NH_4PF_6 (0.40 g, 2.5 mmol) was added to the solution. The brick-red product was collected by filtration, washed with methanol and diethyl ether and dried in vacuo.

3: Yield: 0.449 g, 80% based on Ru(NO)$Cl_3 \cdot 5H_2O$. Anal. Calcd. for $RuC_{10}H_{10}Cl_2F_6N_7OP$: C, 21.40; H, 1.80; N, 17.47. Found: C, 21.50; H, 1.88; N, 17.34%. IR (KBr, cm^{-1}): ν(NO) = 1910. ^{1}H NMR (DMSO-d_6, 298 K): δ 6.81 (pseudo-t,1H, 4-C_B*H*), 6.92 (pseudo-t, 2H, 4-C_A*H*), 8.28 (d, $^3J_{H-H}$ = 2 Hz, 1H, 3 or 5-C_B*H*), 8.46 (d, $^3J_{H-H}$ = 2 Hz, 2H, 3 or 5-C_A*H*), 8.91 (d, $^3J_{H-H}$ = 2 Hz, 1H, 3 or 5-C_B*H*), 9.00 (d, $^3J_{H-H}$ = 2.5 Hz, 2H, 3 or 5-C_A*H*), 10.25 (s, 1H, C*H*). ^{13}C{H} NMR (DMSO-d_6, 298 K): δ 76.37 (*C*H), 109.44 (4-C_BH), 110.29 (4-C_AH), 137.38 (3 or 5-C_BH), 138.49 (3 or 5-C_AH), 147.51 (3 or 5-C_BH), 148.01 (3 or 5-C_AH).

2.5. Synthesis of [(Tpm*)Ru(NO)Cl_2][PF_6] (**4**)

A procedure similar to that described for the preparation of **3** was used, except that during reflux of the solution, a fine pink precipitate formed. It was isolated by filtration and was identified by IR spectrum and NMR as [$(dmpz)_2$Ru(NO)Cl_3] (dmpz = 3,5-dimethylpyrazole) (**5**) [28,48] (0.043 g, yield: 10%). NH_4PF_6 (0.400 g, 2.5 mmol) was then added to the filtrate to give a brown solid, which was collected by filtration, washed with ether and dried in vacuo. Suitable crystals for X-ray diffraction were grown by slow evaporation of an ethanol solution of **4**.

4: Yield: 0.193 g, 30% based on Ru(NO)$Cl_3 \cdot 5H_2O$. Anal. Calc. for $RuC_{16}H_{22}Cl_2F_6N_7OP$: C, 29.78; H, 3.44; N, 15.19. Found: C, 30.11; H, 3.66; N, 14.88%. IR (KBr, cm^{-1}): ν(NO) = 1928. ^{1}H NMR (DMSO-d_6, 298 K): δ 2.69 (s,6H, 3- or 5-C_AH_3), 2.76 (s,3H, 3- or 5-C_BH_3), 2.78 (s,6H, 3- or 5-C_AH_3), 2.80 (s,3H, 3- or 5-C_BH_3), 6.59 (s, 1H, 4-C_B*H*), 6.65 (s, 2H, 4-C_A*H*), 8.08 (s, 1H, C*H*). ^{13}C{H} NMR (DMSO-d_6, 298 K): δ 11.28 (3- or 5-C_AH_3), 12.05 (3- or 5- C_BH_3), 14.67 (3- or 5-C_AH_3), 15.83 (3- or 5- C_BH_3), 69.18 (*C*H), 110.86 (4-C_BH), 110.99 (4-C_AH), 146.10 (3- or 5-C_BCH_3), 146.56 (3- or 5-C_ACH_3), 157.88 (3- or 5-C_ACH_3), 159.23 (3- or 5-C_BCH_3).

2.6. X-ray crystallography

Suitable single crystals of **2** and **4** were mounted on the top of glass fiber for X-ray structure analysis. Diffraction data were collected on a Bruker SMART APEX CCD diffractometer using graphite-monochromatized Mo Kα radiation (λ = 0.71073 Å) at room temperature and corrected for absorption using SADABS program [49]. The structures were solved by direct methods and refined on F^2 against all reflections by full-matrix least-squares methods with SHELXTL program [50]. Anisotropy thermal parameters were assigned to all non-hydrogen atoms.

2.7. Catalytic hydrogen transfer experiments

Under inert atmosphere, the tested complex (0.008 mmol) and KOH (10 mL, 0.02 M in *i*-PrOH), were introduced into a Schlenk tube. The solution was heated to 82 °C for 30 min. Subsequently, ketone (2 mmol) was added. The reaction progress was monitored by GC analysis.

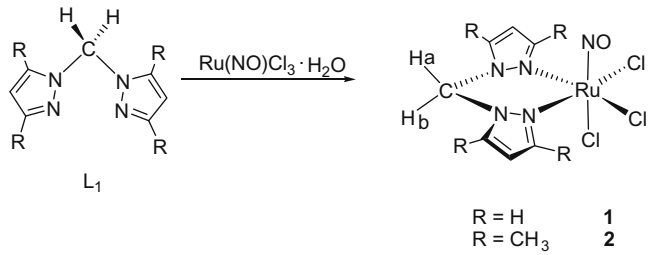

Scheme 1.

3. Results and discussion

3.1. Synthesis and characterization

The synthetic procedures for the new, 18-electron ruthenium(II) nitrosyl complexes $[(L_1)Ru(NO)Cl_3]$ (L_1 = Bpm, **1**; Bpm*, **2**) and $[(L_2)Ru(NO)Cl_2][PF_6]$ (L_2 = Tpm, **3**; Tpm*, **4**) are shown in Schemes 1 and 2, respectively.

Complexes **1** and **2** were obtained by the reaction between $Ru(NO)Cl_3 \cdot 5H_2O$ and ligands Bpm and Bpm*, respectively, in a 1:1 molar ratio. Complexes **4** and **5** were synthesized via the reaction of the ligands Tpm or Tpm*, in a 1:1 molar ratio with $Ru(NO)Cl_3 \cdot 5H_2O$, in the presence of 2.5 equiv. of NH_4PF_6. However, besides **4**, the reaction of $Ru(NO)Cl_3 \cdot 5H_2O$ with Tpm*, also afforded another compound $[(dmpz)_2Ru(NO)Cl_3]$ (dmpz = 3,5-dimethylpyrazole, **5**), which has been previously reported [28,48]. These findings showed that a cleavage of C–N bond occurred in Tpm* to a considerable degree during the reaction of Tpm* with $Ru(NO)Cl_3 \cdot 5H_2O$, affording the carbon-free di-pyrazole complex **5**. The occurrence of the similar cleavage of C–B bond has been observed in the reaction of $RuCl_3(NO)$ and Tp* [28].

The new ruthenium(II) nitrosyl complexes **1–4** are colored and stable in air. **1** and **2** are insoluble in most solvents, while **3** and **4** are soluble in polar organic solvents (DMSO, DMF, CH_3CN). They are diamagnetic, characteristic of the low spin d^6 ruthenium(II) centers in the complexes. The analytical data supported the proposed formulations. In the reactions to yield the complexes, the ligands behave as basic sp^2 N-donors replacing two water molecules and/or one chloride in the ruthenium precursor $Ru(NO)Cl_3 \cdot 5H_2O$.

All four new complexes have been fully characterized by NMR and IR spectra. Only one set of ^1H resonance for the two pyrazolyl rings is observed in **1** or **2**, indicating the two pyrazolyl rings in the complexes are in the same chemical environment, in agreement with the C_s plane of symmetry bisecting the bidentate pyrazolyl ligands. The corresponding resonances due to the methylene backbone protons of the Bpm and Bpm* ligands in **1** and **2** are cleanly split into an AB system at room temperature, indicating that the Ru(Bpm) and Ru(Bpm*) metallacycle in **1** and **2** adopts a rigid conformation [51–53]. It should be noted that variable-temperature ^1H NMR studies show that one hydrogen atom of methylenic CH_2 in **2** at 6.7 ppm is broad at 25 °C and higher temperatures. At lower temperatures, this broad peak graduately changed into a doublet at −10 °C (Fig. 1). This doublet and the doublet at 6.57 ppm for the other H atom in the CH_2 group form an AB system. As noted below, there is an intramolecular hydrogen bond between the nitrogen of nitrosyl group and one hydrogen atom of the CH_2 group, as the X-ray crystal structure of **2** reveals. Since this hydrogen bond is very weak, a possible equilibrium between H-bonded and not H-bonded

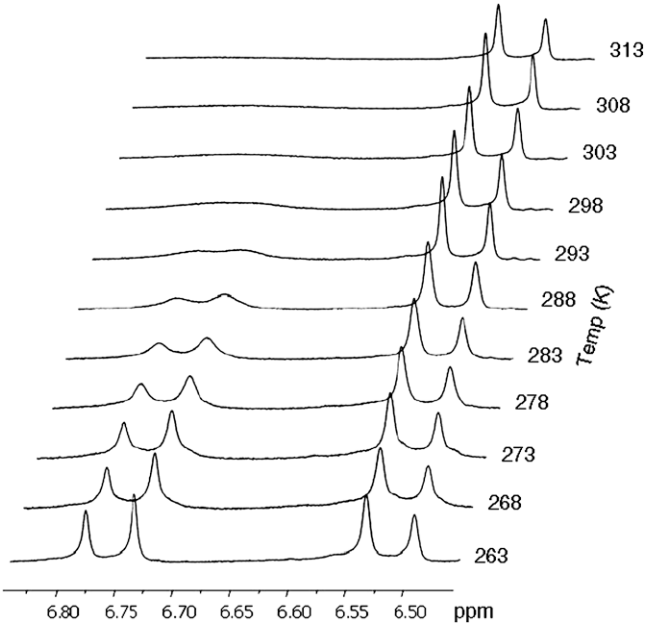

Fig. 1. Variable-temperature ^1H NMR spectra of $[(Bpm^*)Ru(NO)Cl_3]$ (**2**) in DMF-d_7.

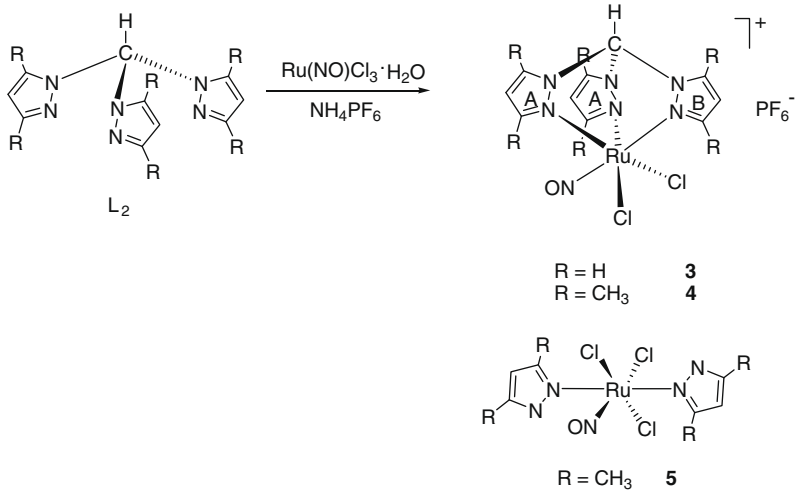

Scheme 2.

species could be involved, which can explain the observed variable-temperature ^{1}H NMR spectra. In the low temperature, the non-bonded species is predominant, which gave a doublet at −10 °C. With the temperature increasing, the equilibrium rate becomes very fast. It is quite possible that with the increasing of temperature, the equilibrium will move to the hydrogen-bonded species. The reason for this equilibrium shift should be due to the thermal motion, which will promote one hydrogen atom of the CH_2 group approach of the nitrogen of nitrosyl group in **2**. In contrast, the same thing did not happen in compound **1**. This may be due to the steric effect of the substituents in pyrazolyl groups. The methyl groups in **2** would promote one hydrogen atom of the CH_2 group approach of the nitrogen of nitrosyl group in **2**, which makes the equilibrium between H-bonded and non H-bonded species possible.

The ^{1}H and ^{13}C NMR spectra clearly show that there are two different chemical environments adopted by the three pyrazolyl rings in **3** and **4**, indicating that two complexes possess mirror symmetry. This observation is consistent with tridentate coordination of Tpm and Tpm* ligands. IR spectra of **1**–**4** gave a sharp, intense band in the range 1870–1928 cm^{-1}, which can be assigned as ν(NO), indicating a linear coordination configuration of the nitrosyl group to Ru [5]. The ν(NO) frequency has been extensively employed to analyze the degree of electronic interaction between the NO ligand and the metal center [1–7]. In nitrosyl complexes with high ν(NO) wavenumbers, the NO$^+$ character is well preserved in a [Ru^{II}–NO$^+$] electronic distribution [6].

3.2. Molecular structures of *2* and *4*

The solid-state structures of **2** and **4** were determined by single-crystal X-ray crystallographic analyses. **4** consists of a well-separated [(Tpm*)Ru(NO)Cl$_2$]$^+$ (**4**$^+$) cation and a PF^-_6 anion. The solid-state structures of **2** and the [(Tpm*)Ru(NO)Cl$_2$]$^+$ cation **4**$^+$ are shown in Figs. 2 and 3, respectively. Crystallographic data for **2** and **4** are presented in Table 1 and selected bond leznghts and angles are given in Table 2.

The coordination geometry of ruthenium in **2** is octahedral with two nitrogen atoms from Bpm*, three chlorine atoms and the nitrogen atom of the NO ligand as the six ligating atoms. The three chlorine atoms adopt the facial configuration and the NO ligand is *trans* to one chlorine atom. The ruthenium is located within the coordination plane defined by Cl(1), Cl(3), N(2), and N(5), as it is situated only 0.035 Å from this plane. The pyrazolyl rings are planar and the

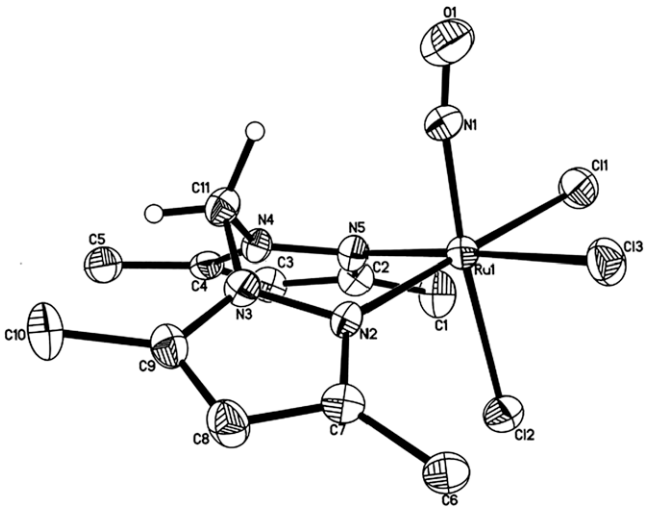

Fig. 2. The ORTEP diagrams of [(Bpm*)Ru(NO)Cl$_3$] (**2**).

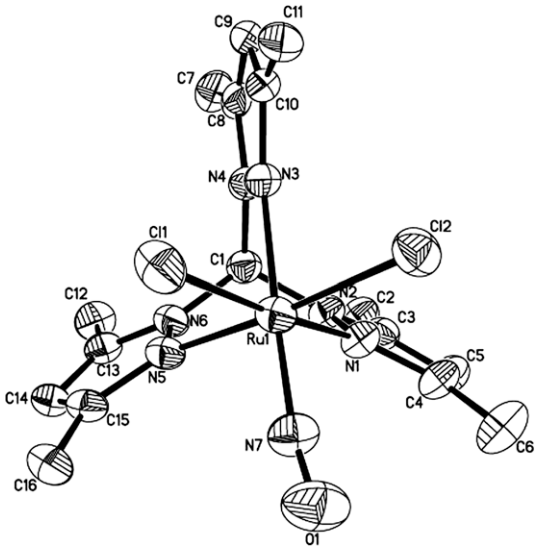

Fig. 3. The ORTEP diagram of [(Tpm*)Ru(NO)Cl$_2$]$^+$ ([**4**]$^+$).

six-membered metallocycle [Ru(N–N)$_2$C] units of the structurally bound Bpm* ligand adopted a pseudo-boat conformation. The Ru–N(ring) bond lengths in **2** [2.117(6) and 2.112(7) Å] are in the range of the reported values [54,55]. The length of the Ru1–Cl2 [2.325(2) Å] bond, the chloride trans to NO, is shorter than the other two Ru–Cl bond lengths [2.355(2) and 2.361(2) Å], suggesting a higher degree of covalency of the Ru–Cl bond trans to NO group. The Ru1–N(nitrosyl) and N–O bond distances are 1.766(8) Å and 1.050(8) Å, respectively, that are comparable with those in other six-coordinate Ru–NO$^+$ type complexes [56,57]. The Ru–N–O angle of 169.4(8)° indicates that the NO group is formally bound as NO$^+$, and this is consistent with the low NO stretching vibration band at 1875 cm^{-1}. There is an intramolecular hydrogen bond between the nitrogen of nitrosyl group and one hydrogen atom of methylene protons of Bpm* ligand [HC–H$\cdots$NO with H$_2$C$\cdots$N(O) 3.077(11) Å] in the solid state in **2**.

[(Tpm*)Ru(NO)Cl$_2$]$^+$ (**4**$^+$) cation exhibits a 6-coordinate octahedral configuration around the ruthenium atom with three nitrogen atoms from Tpm*, two chlorine atoms and one nitrogen atom from nitrosyl ligand. There is a crystallographically imposed mirror plane that includes one pyrazolate ring (trans to the NO$^+$), the Ru center and the NO$^+$ ligand. The pyrazolyl rings within the Tpm* ligand are essentially planar. The N(ring)–Ru–N(ring) angles (from 83.51 to 86.26°) deviate from the values expected for a regular octahedron. Ru–N (ring) bond lengths of av. 2.089 Å are in the range of reported complexes [58–60]. The Ru–Cl1 and Ru–Cl2 bond lengths are 2.3541(18) and 2.3505(19) Å, respectively. The Ru–N(ring) bond (trans to NO) (2.099 Å) is slightly longer than two remaining Ru–N(ring) bonds (2.076 and 2.092 Å). The Ru–N(O) and N(O)–O bond lengths are 1.745(6) Å and 1.076(6) Å, respectively. The Ru–N–O angle of 168.8(6)° is nearly linear.

3.3. Electrochemical study

The cyclic voltammograms of complexes **1**–**4** were carried out at room temperature in DMF solutions at a scan rate of 100 mV s^{-1}. The cyclic voltammograms of **2** and **4** are shown in Fig. 4. The electrochemical behaviors of **1**–**4** are typical for the {Ru^{II}–NO$^+$} complexes [61–64] and the potentials of the redox processes are shown in Table 3. There are two successive reductions waves centered at the coordinated nitrosyl group. The first at the less negative potential (vs. SSCE) is reversible and attributed to the pair Ru^{II}–NO$^+$/Ru^{II}–NO^0. The more negative potential which is irreversible

Table 1
Crystallographic data for [(Bpm*)Ru(NO)Cl3] (**2**) and [(Tpm*)Ru(NO)Cl2](PF6) (**4**)

	2	**4**
Empirical formula	$C_{11}H_{16}Cl_3N_5ORu$	$C_{16}H_{22}Cl_2F_6N_7OPRu$
Formula weight	441.71	645.35
T (K)	291(2)	291(2)
λ (Å)	0.71073	0.71073
Crystal system	Monoclinic	Monoclinic,
Space group	$P\,2_1/n$	$P\,2_1/n$
a (Å)	9.985(3)	13.0211(9)
b (Å)	13.802(4)	10.4571(7)
c (Å)	13.127(4)	18.2153(13)
α (°)	90	90.
β (°)	112.3540(10)	104.6650(10)
γ (°)	90	90
Volume (Å^3)	1673.1(9)	2399.4(3)
Z	4	4
D_{calc} (g/cm^3)	1.754	1.786
Absorption coefficient (mm^{-1})	1.420	1.014
$F(000)$	880	1288
Crystal size (mm^3)	0.30 × 0.26 × 0.24	0.28 × 0.24 × 0.19
θ Range for data collection (°)	2.21–26.00	2.21–25.99
Index ranges	$-11 \leqslant h \leqslant 12$, $-17 \leqslant k \leqslant 9$, $-15 \leqslant l \leqslant 16$	$-16 \leqslant h \leqslant 15$, $-12 \leqslant k \leqslant 12$, $-13 \leqslant l \leqslant 22$
Reflections collected	8627	12917
Independent reflections (R_{int})	3288 [R_{int} = 0.0767]	4714 [R_{int} = 0.0681]
Completeness to θ = 26.00 (%)	99.8	99.8
Max. and min. transmission	0.705 and 0.654	0.8307 and 0.7644
Data/restraints/parameters	3288/10/194	4714/2/313
GOF	1.016	1.001
Final R indices [$I > 2\sigma(I)$][a]	R_1 = 0.0400, wR_2 = 0.0544	R_1 = 0.0482, wR_2 = 0.0936
R indices (all data)	R_1 = 0.0723, wR_2 = 0.0584	R_1 = 0.0938, wR_2 = 0.1230
Largest differences in peak and hole (e Å^{-3})	0.554 and −0.636	0.591 and −0.665

[a] $R1 = \Sigma||F_o| - |F_c||/\Sigma|F_o|$; $wR_2 = [\Sigma w(|F_o| - |F_c|)^2/\Sigma w|F_o|^2]^{1/2}$; GOF = $[\Sigma w(|F_o| - |F_c|)^2/(n_o - n_v)]^{1/2}$.

Table 2
Selected bond distances (Å) and angles (°) for [(Bpm*)Ru(NO)Cl3] (**2**) and [(Tpm*)Ru(NO)Cl2][PF6] (**4**)

2			
Ru1–Cl1	2.355(2)	Ru1–N2	2.117(6)
Ru1–Cl2	2.325(2)	Ru1–N5	2.112(7)
Ru1–Cl3	2.361(2)	N1–O1	1.050(8)
Ru1–N1	1.766(8)		
N1–Ru1–N5	97.6(3)	N5–Ru1–N2	87.3(3)
N1–Ru1–N2	94.3(3)	N5–Ru1–Cl1	93.23(19)
N1–Ru1–Cl1	86.3(2)	N5–Ru1–Cl2	87.9(2)
N1–Ru1–Cl2	174.0(3)	N5–Ru1–Cl3	177.0(2)
N1–Ru1–Cl3	85.4(3)	Cl1–Ru1–Cl2	91.02(8)
N2–Ru1–Cl1	179.2(2)	Cl1–Ru1–Cl3	86.93(9)
N2–Ru1–Cl2	88.41(18)	Cl2–Ru1–Cl3	89.12(9)
N2–Ru1–Cl3	92.46(19)	O1–N1–Ru1	169.4(8)
4			
Ru1–N1	2.076(5)	Ru1–Cl1	2.3541(18)
Ru1–N3	2.098(5)	Ru1–Cl2	2.3505(19)
Ru1–N5	2.093(5)	N7–O1	1.076(6)
Ru1–N7	1.745(6)		
N1–Ru1–N3	83.5(2)	N3–Ru1–Cl2	88.59(15)
N1–Ru1–N5	86.2(2)	N5–Ru1–Cl1	91.77(14)
N1–Ru1–N7	94.0(2)	N5–Ru1–Cl2	173.89(14)
N1–Ru1–Cl1	174.09(15)	N7–Ru1–N5	95.2(2)
N1–Ru1–Cl2	90.98(15)	N7–Ru1–Cl1	91.8(2)
N3–Ru1–N5	85.69(19)	N7–Ru1–Cl2	90.45(19)
N3–Ru1–N7	177.3(2)	Cl1–Ru1–Cl2	90.45(7)
N3–Ru1–Cl1	90.79(15)	O1–N7–Ru1	168.8(6)

corresponds to the Ru^{II}–NO^0/Ru^{II}–NO^- process. It is well-known that the nitrosyl ligand shows a strong interaction with the ligand at the trans position by sharing the same d orbital in the coordination sphere, so that the $E(Ru^{II}–NO^+/Ru^{II}–NO^0)$ redox potentials span a broad range and are very sensitive to the degree of $d\,\pi$–$p\,\pi^*$ backbonding between the metal and the nitrosyl group [65]. For complexes **1–4**, as with the IR ν(NO) frequencies (Table 3), redox potentials provide information about the electronic nature of the

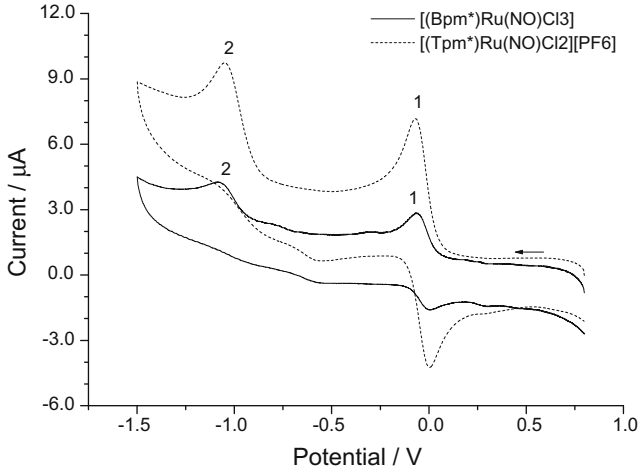

Fig. 4. Cyclic voltammograms of complexes [(Bpm*)Ru(NO)Cl3] (**2**) and [(Tpm*)Ru(NO)Cl2][PF6] (**4**).

Table 3
Infrared data and redox potentials for **1–4**

Complex	ν(NO) cm^{-1}	$E_{1/2}(1)$[a]	$E_{pc}(2)$[b]
[Ru(NO)(Bpm)Cl3] (**1**)	1870	−0.37	−0.91
[Ru(NO)(Bpm*)Cl3(**2**)	1875	−0.03	−1.08
[Ru(NO)(Tpm)][PF6] (**3**)	1911	−0.07	−0.86
[Ru(NO)(Tpm*)Cl2][PF6] (**4**)	1928	−0.04	−1.05

[a] $E_{1/2}(1)$ is the first nitrosyl-based reduction and is electrochemically reversible ($Ru^{II}–NO^+/Ru^{II}–NO^0$).

[b] $E_{pc}(2)$ is the peak potential for the second nitrosyl-based reduction (($Ru^{II}–NO^0$/$Ru^{II}–NO^{-1}$). The process is electrochemically irreversible.

compound. High redox potentials correlate with high NO stretching frequencies and reflect a smaller degree of metal-to-nitrosyl back-bonding. Compared with the reduction potential for the $[RuCl(NO)(bipy)_2][PF_6]_2$ ($E_{1/2}$ = −0.20 V) [52], our complexes ($E_{1/2}$ = −0.37 ∼ −0.03 V) shows some degree of $d\ \pi$–$p\ \pi^*$(NO) back-donation. The degree order is **2** > **4** > **3** > $[RuCl(NO)(bipy)_2]$-$[PF_6]_2$ > **1**.

3.4. Catalytic hydrogenation of ketones

The classical transfer hydrogenation of acetophenone by isopropanol was used as a model reaction to explore the catalytic behavior of complexes **1–4** in transfer hydrogenation. The catalytic tests were carried out using the ruthenium catalyst precursors **1–4** (0.4 mol%), KOH (10 mol%) and acetophenone (2 mmol) in 10 mL ^{i}PrOH at 82 °C (Eq. (1)). The reaction was monitored by gas chromatography. The conversion vs. time plots for the four precursor catalysts **1**–**4** are shown in Fig. 5. The following features deserve comments: (i) There is a strong influence of the methyl substituents in the pyrazolyl groups on the catalytic activity, increasing in the order **2** > **1**, **4** > **3**, and **2** is the most efficient in the transfer hydrogenation of acetophenone to 1-phenylethanol. The relative activity order suggests that sterically bulky ligand is superior. Noyori and co-workers [66] have shown that the true catalyst in the hydrogenation reaction is formally a 16-e intermediate species. It is possible that the bulky ligands help the formation of stable of 16-e intermediates, thus increasing the activities of this hydrogenation process [67,68]. (ii) The catalytic performances shown by complexes **1–2** containing bidentate L_1 ligands (Scheme 1) are, in all cases, better than those of counterparts **3–4** with tridentate L_2 ligands (Scheme 2). The lower activities of **3** and **4** may be due to the presence of anion PF^-_6 in the complexes [69,70]. The underlying reasons of these differences remain to be elucidated.

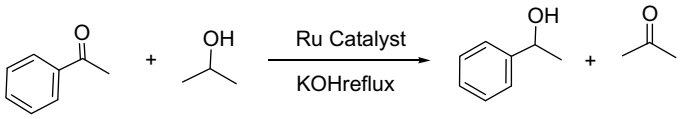

(1)

The most active complex **2** has also been tested in the transfer hydrogenation of other ketones (Table 4). As in the case of acetophenone (entry 1 and Fig. 5), **2** exhibits a considerable efficiency for transfer hydrogenation of 4'-chloroacetophenone (83% conversion after 6 h, entry 2), 4'-methoxyacetophenone (67% conversion after 6 h, entry 3), and diphenyketone (78% conversion after 6 h, entry 4). **2** was found to be a particularly efficient catalyst in the reduction of diakyl ketones. The conversions of cyclohexanone and 2-heptanone are as high as 95 and 94% after 6 h of reaction (entries 6 and 7). But the catalytic activity is significantly low in the case of 2,4,6-trimethyl-acetophenone (conversion 11% after 6 h, entry 5). This may be due to steric effect of this substrate, which restricts the formation of the catalytic 16-e intermediate.

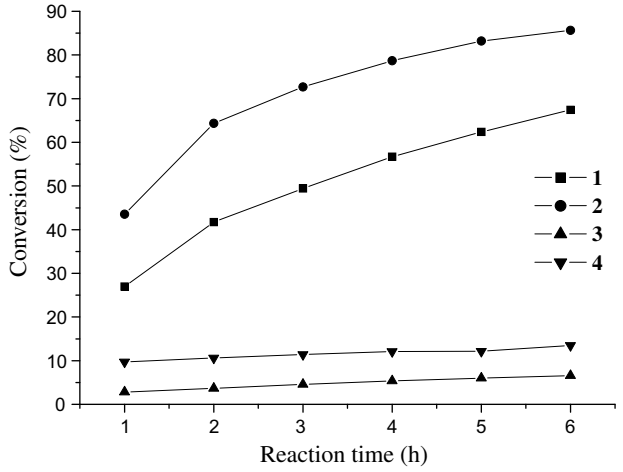

Fig. 5. Conversion vs. reaction time for conditions given in Section 2. Precursor catalyst systems shown are for **1–4**.

Table 4
Catalytic transfer hydrogenation of ketones using **2**[a]

Entry	Substrate	Product	Time (h)	Conversion%[b]
1	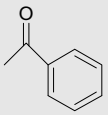	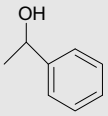	1 6	43 86
2	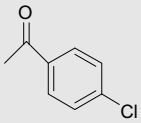	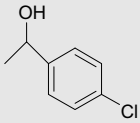	1 6	45 83
3	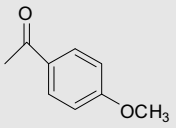	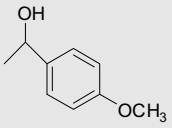	1 6	37 67
4	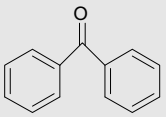	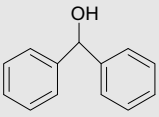	1 6	44 78
5	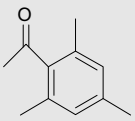	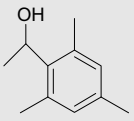	1 6	3 11
6	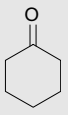	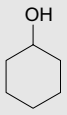	1 6	69 95
7	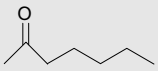	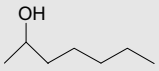	1 6	58 94

[a] Conditions: reactions were carried out at 82 °C, ketone 0.2 M in 2-propanol, ketone/Ru/KOH = 1000/4/100.
[b] The conversion was determined by GC.

4. Conclusions

New ruthenium nitrosyl complexes **1**–**4** bearing polypyrazolylmethane ligands such as Bpm, Bpm*, Tpm, and Tpm* ligands have been prepared and characterized. Molecular structures of **2** and **4** show that the bidentate and tridentate coordination of the Bpm* and Tpm* ligands to ruthenium atom, respectively. The study of the transfer hydrogenation of acetophenone indicated that **2** is the most efficient, suggesting that bulky substit-

uents are superior. The role of nitrosyl ligand in this catalytic conversion is not clear yet, which need to be studied in future.

Acknowledgements

This work was supported by National Basic Research Program of China (No. 2006CB806104 and 2007CB925102), Natural Science Grant of China (No. 20721002 and 50572037), and the US National Science Foundation.

Appendix A. Supplementary data

CCDC 695577 and 695848 contain the supplementary crystallographic data for complexes **2** and **4**. These data can be obtained free of charge from the Cambridge Crystallographic Data Centre via www.ccdc.cam.ac.uk/data_request/cif. Supplementary data associated with this article can be found, in the online version, at doi:10.1016/j.jorganchem.2008.09.045.

References

[1] G.B. Richter-Addo, P. Legzdins, Metal Nitrosyls, Oxford University Press, New York, 1992.
[2] G.B. Richer-Addo, P. Legzdins, Chem. Rev. 88 (1988) 991.
[3] T.W. Hayton, P. Legzdins, W.B. Sharp, Chem. Rev. 102 (2002) 935.
[4] J.A. McCleverty, Chem. Rev. 104 (2004) 403.
[5] F. Bottomley, Coord. Chem. Rev. 26 (1978) 7.
[6] J.H. Enemark, R.D. Feltham, Coord. Chem. Rev. 13 (1974) 339.
[7] E. Tfouni, M. Krieger, B.R. McGarvey, D.W. Franco, Coord. Chem. Rev. 236 (2003) 57.
[8] S. Kuwata, S. Kura, T. Ikariya, Polyhedron 26 (2007) 4659.
[9] Á. Kathó, Z. Opre, G. Laurenczy, F. Joó, J. Mol. Catal. A: Chem. 204–205 (2003) 143.
[10] S.T. Wilson, J.A. Osborn, J. Am. Chem. Soc. 93 (1971) 3068.
[11] H. Lebel, V. Paquet, Organometallics 23 (2004) 1187.
[12] G. Zassinovich, G. Mestroni, S. Gladiali, Chem. Rev. 92 (1992) 1051.
[13] R. Noyori, S. Hashiguchi, Acc. Chem. Res. 30 (1997) 97.
[14] J.-E. Bäckvall, J. Organomet. Chem. 652 (2002) 105.
[15] T. Ikariya, A.J. Blacker, Acc. Chem. Res. 40 (2007) 1300.
[16] S. Gladiali, E. Alberico, Chem. Soc. Rev. 35 (2006) 226.
[17] D. Cuervo, M.P. Gamasa, J. Gimeno, Chem. Eur. J. 10 (2004) 425.
[18] X.J. Sun, H.X. Deng, Z.K. Yu, J.H. Dong, S.Z. Wu, Organometallics 24 (2005) 4110.
[19] F.L. Zeng, Z.K. Yu, Organometallics 27 (2008) 289.
[20] Z.K. Yu, F.L. Zeng, X.J. Sun, H.X. Deng, J.H. Dong, J.Z. Chen, H.M. Wang, C.X. Pei, J. Organomet. Chem. 692 (2007) 2306.
[21] W.Q. Ta, X.D. Zhao, Z.K. Yu, J. Organomet. Chem. 692 (2007) 5395.
[22] S. Trofimenko, Chem. Rev. 93 (1993) 943.
[23] H. Cai, W.H. Lam, X.-H. Yu, X.-Z. Liu, Z.-Z. Wu, T.-N. Chen, Z.-Y. Lin, X.-T. Chen, X.-Z. You, Z.-L. Xue, Inorg. Chem. 42 (2003) 3008.
[24] C. Slugovc, R. Schmid, K. Kirchner, Coord. Chem. Rev. 185–186 (1999) 109.
[25] L.A. Goj, M. Lail, K.A. Pittard, K.C. Riley, T.B. Gunnoe, J.L. Petersen, Chem. Commun. (2006) 982.
[26] J.P. Lee, J.O.C. Jimenez-Halla, T.R. Cundari, T.B. Gunnoe, J. Organomet. Chem. 692 (2007) 2175.
[27] Y. Feng, M. Lail, K.A. Barakat, T.R. Cundari, T.B. Gunnoe, J.L. Petersen, J. Am. Chem. Soc. 127 (2005) 14174.
[28] M. Onishi, Bull. Chem. Soc. Jpn. 64 (1991) 3039.
[29] Y. Arikawa, Y. Nishimura, H. Kawano, M. Onishi, Organometallics 22 (2003) 3354.
[30] Y. Arikawa, Y. Nishimura, K. Ikeda, M. Onishi, J. Am. Chem. Soc. 126 (2004) 3706.
[31] Y. Nishimura, Y. Arikawa, T. Inoue, M. Onishi, Dalton Trans. (2005) 930.
[32] Y. Arikawa, T. Asayama, M. Onishi, J. Organomet. Chem. 692 (2007) 194.
[33] Y. Arikawa, K. Ikeda, T. Asayama, Y. Nishimura, M. Onishi, Chem. Eur. J. 13 (2007) 4024.
[34] Y. Arikawa, T. Asayama, Y. Moriguchi, S. Agari, M. Onishi, J. Am. Chem. Soc. 129 (2007) 14160.
[35] Y. Arikawa, T. Asyama, C. Tanaka, S. Tashita, M. Tsuji, K. Ikeda, K. Umkoshi, M. Onishi, Organometallics 27 (2008) 1227.
[36] H.R. Bigmore, S.C. Lawrence, P. Mountford, C.S. Tredget, Dalton Trans. (2005) 635.
[37] D.L. Reger, Comments Inorg. Chem. 21 (1999) 1.
[38] L.D. Field, B.A. Messerle, L. Soler, I.E. Buys, T.W. Hambley, J. Chem. Soc. Dalton Trans. (2001) 1959.
[39] W.W. Volcheck, D.A. Tocher, W.E. Geiger, J. Organomet. Chem. 692 (2007) 3300.
[40] S. Bhanbri, D.A. Tocher, J. Chem. Soc. Dalton Trans. (1997) 3367.
[41] A. Macchioni, G. Bellachioma, G. Cardaci, G. Cruciani, E. Foresti, P. Sabatino, C. Zuccaccia, Organometallics 17 (1998) 5549.
[42] H.S. Chu, Z.T. Xu, S.M. Ng, C.P. Lau, Z.Y. Lin, Eur. J. Inorg. Chem. (2000) 993.
[43] M. Yamaguchi, T. Iida, T. Yamagishi, Inorg. Chem. Commun. 1 (1998) 299.
[44] M. Videla, J.S. Jacinto, R. Baggio, M.T. Garland, P. Singh, W. Kaim, L.D. Slep, J.A. Olabe, Inorg. Chem. 45 (2006) 8608.
[45] A.S. Potapov, A.I. Khlebnikov, Polyhedron 25 (2006) 2683.
[46] D.L. Reger, T.C. Grattan, K.J. Brown, C.A. Little, J.J.S. Lamba, A.L. Rheingold, R.D. Sommer, J. Organomet. Chem. 607 (2000) 120.
[47] C.F. Fortney, R.E. Shepherd, Inorg. Chem. Commun. 7 (2004) 1065.
[48] D.S. Bohle, E.S. Sagan, Eur. J. Inorg. Chem. (2000) 1609.
[49] G.M. Sheldrick, Program for Empirical Absorption Correction, University of Göttingen, Germany, 2000.
[50] G.M. Sheldrick, Program for Crystal Structure Solution and Refinement, University of Göttingen, Germany, 2000.
[51] O. Juanes, J. Mendoza, J.C. Rodríguez-Ubis, J. Organomet. Chem. 363 (1989) 393.
[52] G. Sánchez, J.L. Serrano, J. Pérez, M.C.R. Arellano, G. López, E. Molins, Inorg. Chim. Acta 295 (1999) 136.
[53] L.D. Field, B.A. Messerle, M. Rehr, L.P. Soler, T.W. Hambley, Organometallics 22 (2003) 2387.
[54] S. Huh, Y. Kim, S. PARK, T-J. PARK, M-J. Jun, Acta Cryst. Sect. C 55 (1999) 850.
[55] M.O. Albers, S.F.A. Crosby, D.C. Liles, D.J. Robinson, A. Shaver, E. Singleton, Organometallics 6 (1987) 2014.
[56] G.V. Poelhsitz, R.C. Lima, R.M. Carlos, A.G. Ferreira, A.A. Batista, A.S. Araujo, J. Ellena, E.E. Castellano, Inorg. Chim. Acta 359 (2006) 2896.
[57] R.C.L. Zampieri, G.V. Poelhsitz, A.A. Batista, O.R. Nascimento, J. Ellena, E.E. Castellano, J. Inorg. Biochem. 92 (2002) 82.
[58] D.L. Reger, R.F. Semeniuc, C. Pettinari, F. Luna-Giles, M.D. Smith, Cryst. Growth Des. 6 (2006) 1068.
[59] C. Metcalfe, H. Adams, I. Haq, J.A. Thomas, Chem. Commun. (2003) 1152.
[60] S. Bhambri, D.A. Tocher, Polyhedron 15 (1996) 2763.
[61] D.W. Pipes, T.J. Meyer, Inorg. Chem. 23 (1984) 2466.
[62] R.W. Callahan, T.J. Meyer, Inorg. Chem. 16 (1977) 574.
[63] G.V. Poelhsitz, A.A. Batista, J. Ellena, E.E. Castellano, E.S. Lang, Inorg. Chem. Commun. 8 (2005) 805.
[64] S. Sarkar, B. Sarkar, N. Chanda, S. Kar, S.M. Mobin, J. Fiedler, W. Kaim, G.K. Lahiri, Inorg. Chem. 44 (2005) 6092.
[65] B.J. Coe, S.J. Glenwright, Coord. Chem. Rev. 203 (2000) 5. and references therein.
[66] K.J. Haack, S. Hashiguchi, A. Fujii, T. Ikariya, R. Noyori, Angew. Chem. Int. Ed. Engl. 36 (1997) 285.
[67] V. Cadierno, P. Crochet, J. Diez, S.E. Garcia-Garrido, J. Gimeno, Organometallics 23 (2004) 4836.
[68] R.K. Rath, M. Nethaji, A.R. Chakravarty, Polyhedron 20 (2001) 2735.
[69] J.R. Miecznikowski, R.H. Crabtree, Polyhedron 23 (2004) 2857.
[70] M.P. Araujo, A.T. Figueiredo, A.L. Bogado, G.V. Poelhsitz, J. Ellena, E.E. Castellano, C.L. Donnici, J.V. Comasseto, A.A. Batista, Organometallics 24 (2005) 6159.